

Case Report
Open Access

Multiple Traumatic Fat Embolism with Aortic Dissection III A Case Report

Hui Hua Hu*, Wenguo Wang, Yuqing Huang and Xiaocong Wang

Department of ICU, Suizhou Hospital, Hubei University of Medicine, Suizhou, Hubei, China

ABSTRACT

Multiple trauma refers to the severe injury of multiple body parts caused by a single injury factor, occurring simultaneously or consecutively. This condition leads to numerous tissue injuries, significant organ damage, and high mortality rates. Fat embolism syndrome, on the other hand, is a clinical condition marked by the presence of fat droplets in the bloodstream, resulting in a range of symptoms and signs. The most prevalent manifestations include ecchymotic rash, respiratory distress, and neurological dysfunction. In intensive care units (ICUs), routine CT scans are essential, particularly chest CTs, which often reveal a diffuse distribution of ground glass opacity shadows. In more extensive cases, “snowstorm”-like changes may be observed. Traumatic aortic injuries frequently manifest as scissor force injuries at the aortic isthmus, with the majority of cases occurring in this region. However, other aortic injuries typically occur at the aortic hiatus and the origins of major vessels. Instances where both fat embolism and traumatic aortic dissection III occur concurrently due to multiple trauma are exceptionally rare.

***Corresponding author**

Huihua HU, Department of ICU, Suizhou Hospital, Hubei University of Medicine, Suizhou, Hubei, China.

Received: June 18, 2024; **Accepted:** June 21, 2024; **Published:** July 05, 2024

Keywords: Multiple Trauma, Fat Embolism, Aortic Dissection III, CT, CTA; Long Bone Fracture

List of Abbreviations

CT: computerized tomography

CTA: computerized tomography artery

CVP: Central Venous Pressure

ECG: Electrocardiograph

Case Presentation

A case of multiple traumatic fat embolism with aortic dissection type III is presented here. Upon admission, the patient exhibited severe trauma to the right lower extremity, accompanied by multiple glass grinding nodules. Imaging studies revealed a slightly widened pulmonary artery and a flaky low-density shadow in the left occipito-parietal lobe of the brain. Notably, the right atrium was enlarged, with a transverse diameter of approximately 41mm. Subsequent computed tomography (CT) scans demonstrated a significant widening of the pulmonary artery. A pulmonary CTA review confirmed embolization in the right upper lobe branch of the pulmonary artery, along with a thickened main pulmonary artery, measuring approximately 3.3cm in diameter. However, it was observed that the area of pulmonary thrombus did not correlate precisely with the thickening of the main pulmonary artery. These findings supported a clear diagnosis of fat embolism in the patient. Furthermore, mediastinal CT scans indicated calcification in the descending aorta, raising suspicion of endometrial shedding. On May 13 CTA with 3D reconstruction and imaging of the thoracic and abdominal aorta revealed the presence of aortic dissection, specifically type III. This case highlights the complexity and urgency of managing patients with multiple traumatic injuries,

particularly when complicated by fat embolism and aortic dissection. Prompt diagnosis and treatment are crucial to optimize patient outcomes.

Conclusions

Cases involving both fat embolism and aortic dissection type III due to multiple trauma are indeed rare, posing significant challenges in treatment and often resulting in a poor prognosis. The complexity of these injuries, coupled with their rarity, demands a high level of medical expertise and swift intervention to optimize patient outcomes.

Case

Patient, male, 58 years old, He was admitted to our hospital on May 9, 2024, at 16:30, presenting with “three hours of consciousness disturbance following multiple bodily injuries and trauma to the right lower limb.” Upon admission to the Trauma Orthopedics Emergency Department, a CT scan [Figure 1, Figure 2, Figure 3, Figure 4]. revealed the following findings: Head: The plain CT scan did not detect any obvious traumatic changes. Chest: A pulmonary bulla was identified in the upper lobe of the right lung. Bilateral superior septal emphysema and lung contusion in the lower lobes of both lungs were observed. Multiple ground glass nodules were found in the lower lobes of both lungs, with the largest nodule located in the left lower lobe (size approximately 33mm×29mm). Short-term reexamination is recommended to exclude any space-occupying lesions. Multiple solid nodules were also present in the lower lobe of the right lung, with the largest nodule located in the right lower lobe (size approximately 12mm×11mm). Rib fractures were noted on both sides, as well as fractures of thoracic vertebrae 4 and 12. Mediastinal and bilateral

axillary lymph nodes were visible. Slight thickening of the lower esophageal wall was detected. Coronary artery calcification was present. The aorta and a portion of the thoracic aorta tube wall exhibited thickening and blurring, possibly due to injury. If necessary, a CTA examination is recommended. Abdomen: A small amount of blood was detected around the liver, suggesting the need for follow-up to rule out liver injury. Thickening of the diaphragm in the right costophrenic angle was noted. A left kidney cyst, approximately 2.1cm in diameter, was also observed. Soft tissue swelling and blurred subcutaneous fat space were evident in the right anterior lower abdominal wall. Pelvis: No obvious fracture signs were seen in the pelvis, though some artifacts were present. A follow-up review is recommended. Right Tibia and Fibula: A comminuted fracture was identified in the lower segment of the right tibia and fibula. The broken ends were displaced, and the surrounding soft tissue was swollen, with pneumatosis.

The treatment protocol entailed emergency endotracheal intubation, ventilator-assisted breathing, and continuous ECG monitoring upon admission. To further assess the patient's condition, comprehensive blood tests, biochemistry profiles, coagulation studies, PCT, and ECG were promptly conducted. Rescue measures such as central venous catheterization (CVP 17.6mmH₂O), fluid resuscitation, shock management, tetanus prophylaxis, acid-base balance correction, antibiotic therapy, expectorant administration, acid inhibition, and gastric mucosa protection were initiated. The trauma team oversaw the management, closely monitoring the fluctuations in the patient's vital signs, and actively maintaining them within normal ranges. From 18:30 to 20:40 on May 9, 2024, surgical interventions were performed, including debridement and suturing of the right calf, left elbow, and left hand; amputation of the right calf; and application of an external fixator to the right femur. He underwent a CT scan On May 10 [Figure5, Figure6, Figure7, Figure8] and his heart color ultrasound revealed the presence of numerous back bleeding signals during systole of the tricuspid valve opening, along with an enlarged right atrium (approximately 41mm in diameter). No evident venous thrombosis was observed in both lower limbs, although the deep veins exhibited a hypercoagulable

state. He underwent a CT scan On May 12 [Figure9], On May 12 at 18:00, the patient developed high fever (38.4°C) accompanied by low blood pressure. Another plain CT scan was conducted on May 13 [Figure10]. On the same day at 21:00, due to decreased oxygen levels and blood pressure, abdominal distension occurred and subsequently an enema was performed followed by a CT examination [Figure11, Figure12, Figure13] at 22:00. Cardiac color ultrasound on May 14 indicated enlargement of both the right atrium (transverse diameter approximately 48mm) and right ventricle (transverse diameter approximately 46mm). A significant number of back bleeding signals were observed during systole of the tricuspid valve opening. The patient experienced fever with low blood pressure on both May 13 and May 14; non-invasive cardiac function examination showed high volute and low resistance indicative of septic shock. Despite active anti-infection treatment being administered to the patient, sudden cardiac arrest occurred on May 15 leading to his demise.



Figure 1: X-Ray Examination on Admission on May 9

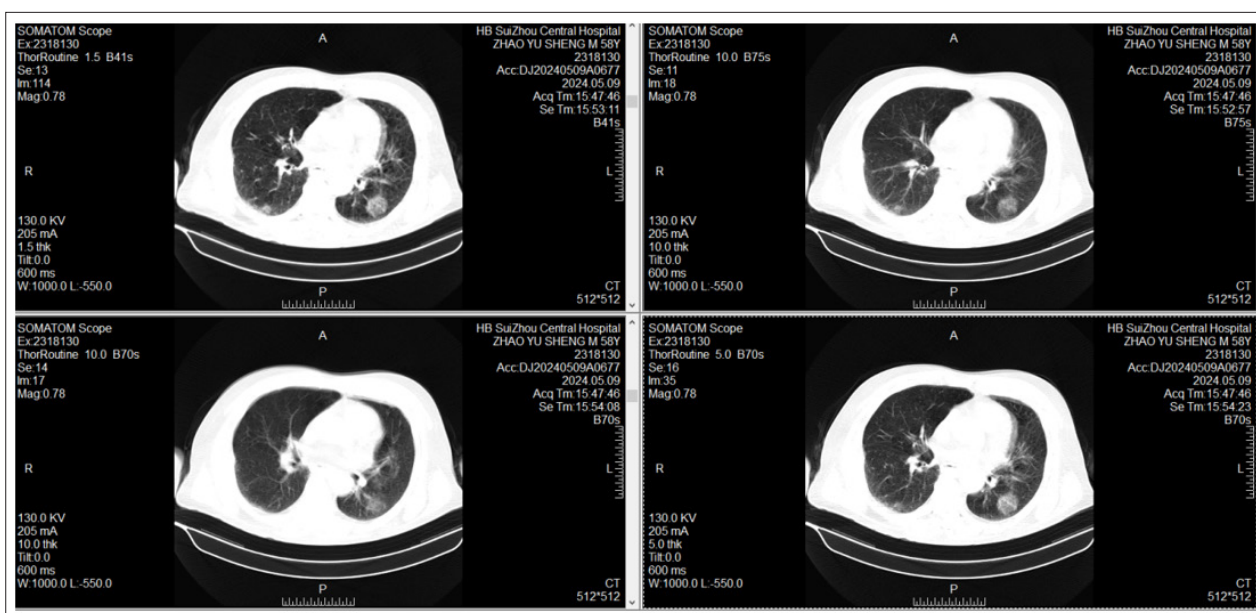


Figure 2: Lung CT examination on admission on May 9: Multiple ground glass nodules were found in the lower lobe of both lungs (IM121, IM159, IM112, IM138). The larger one was located in the left lower lobe of the lung (IM112), with a size of about 33mm×29mm. Short-term reexamination was recommended to exclude space occupying. Multiple solid nodules were found in the

lower lobe of the right lung (IM115, IM134), the larger one was located in the lower lobe of the right lung (IM115), the size of which was about 12mm×11mm.

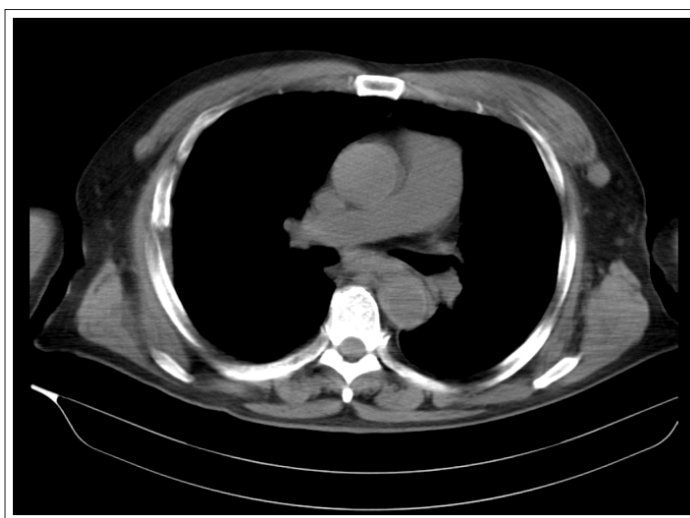


Figure 3: Mediastinum CT examination on admission on May 9: Slightly wider pulmonary artery

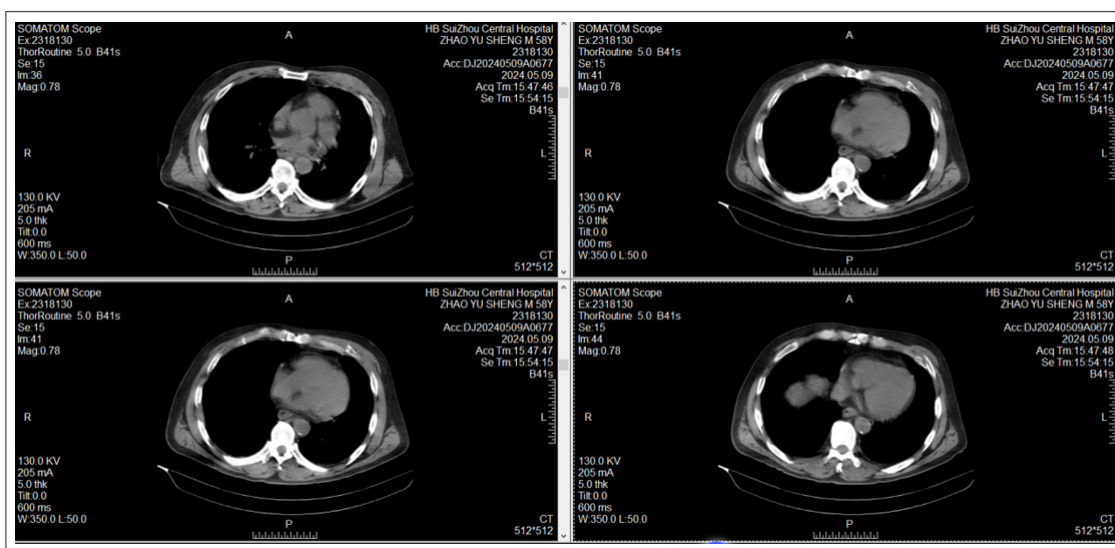


Figure 4: Mediastinum CT examination on admission on May 9: Calcification in descending aorta, suspected endometrium shedding

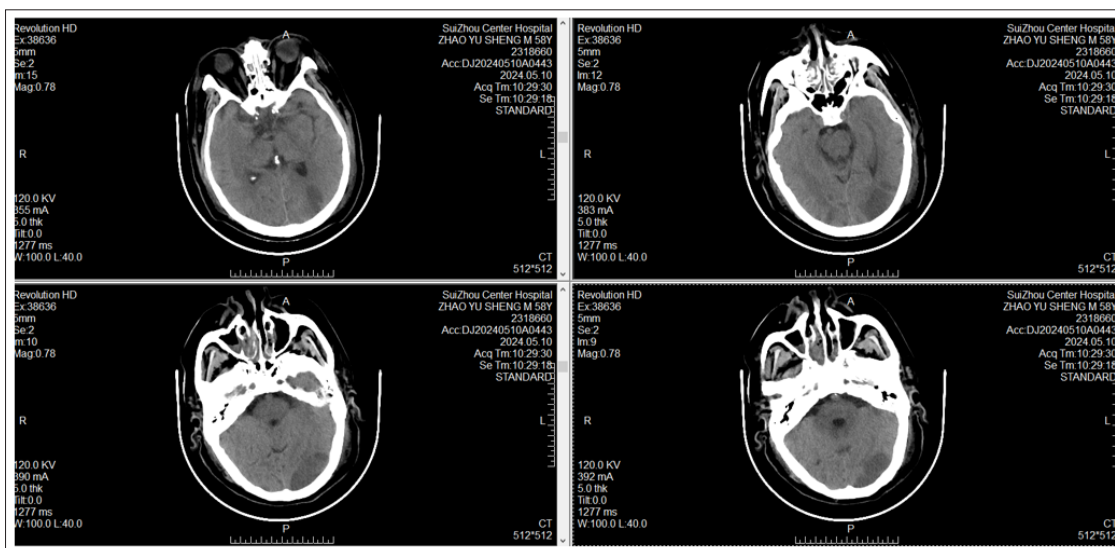


Figure 5: Craniocerebral CT examination on May 10: The left occipito-parietal lamellar low-density shadow is considered cerebral infarction.

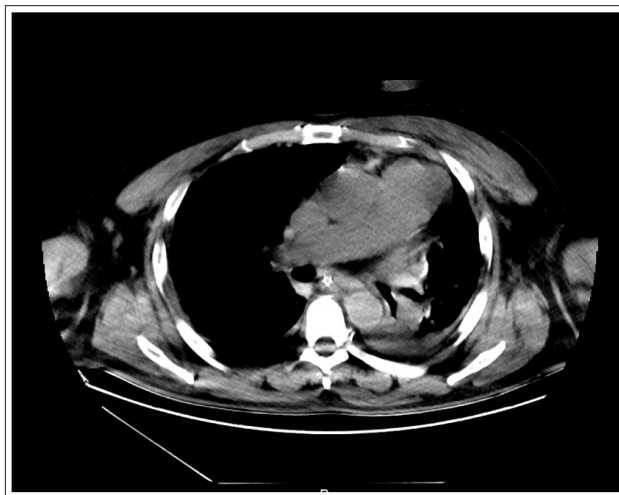


Figure 6: Mediastinal CT on May 10 showed that the pulmonary artery was wider than that on May 9

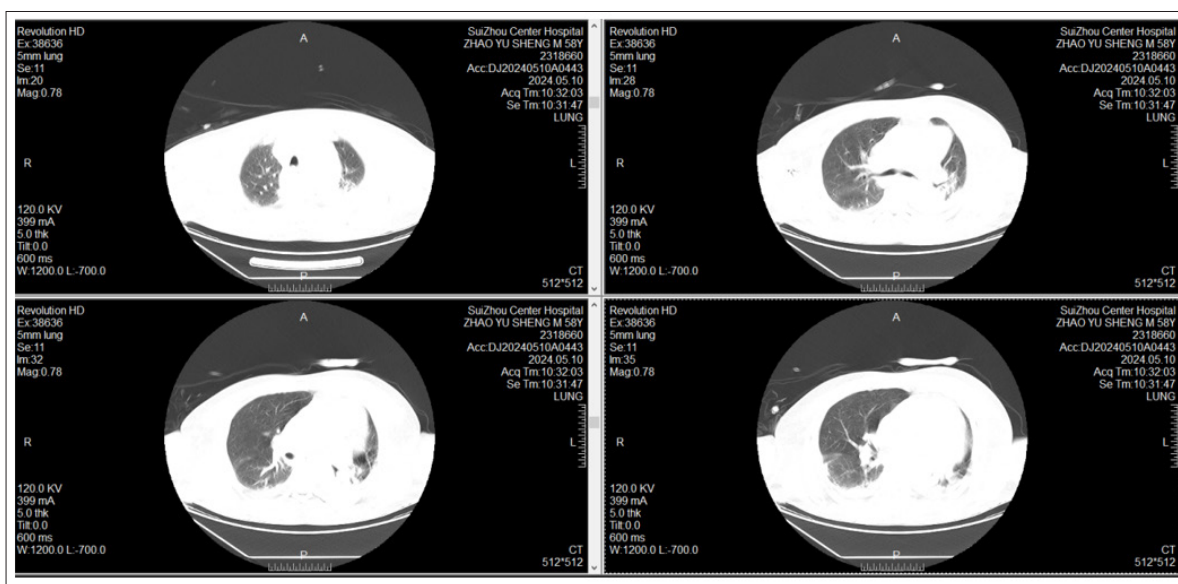


Figure 7: Lung CT on May 10 showed multiple ground glass nodules without obvious nodules in the lower lobes of both lungs

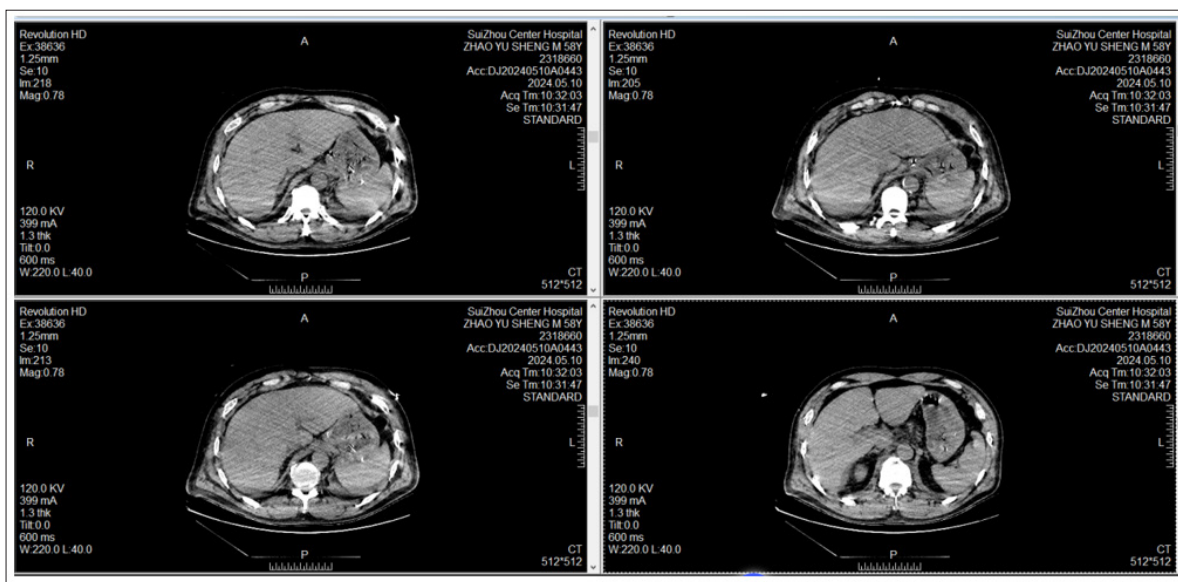


Figure 8: CT on May 10 showed calcification and suspicious dissection in the descending aorta.Lower abdominal and pelvic effusion (hematosis), compared with May 9, new, it is recommended to combine clinical and review

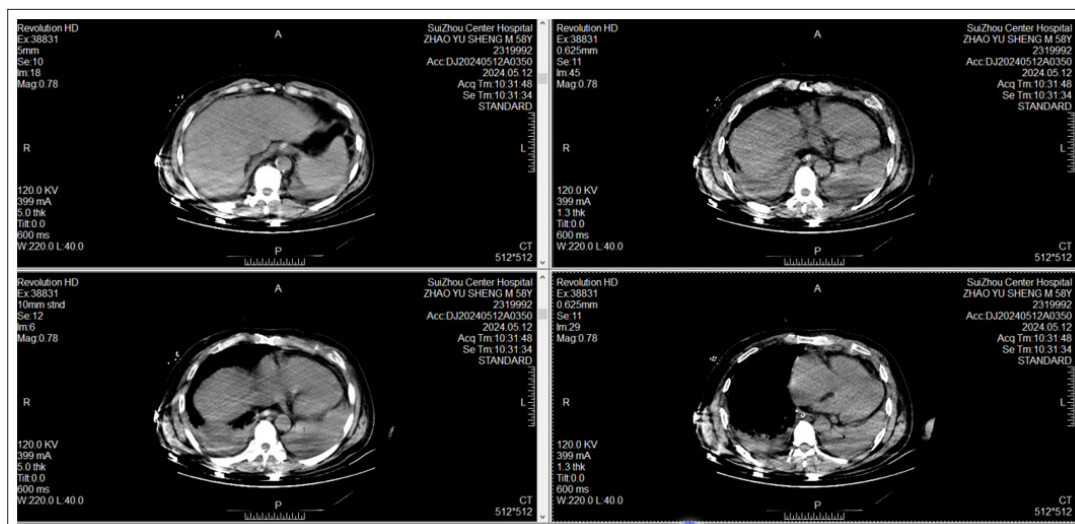


Figure 9: CT on May 12 showed calcification and suspicious dissection in the descending aorta. Lower abdominal and pelvic effusion (hematosis), similar to the ratio of May 10, it is recommended to combine clinical and review



Figure 10: Mediastinal CT on May 13 showed that the pulmonary artery was similar to that on on May

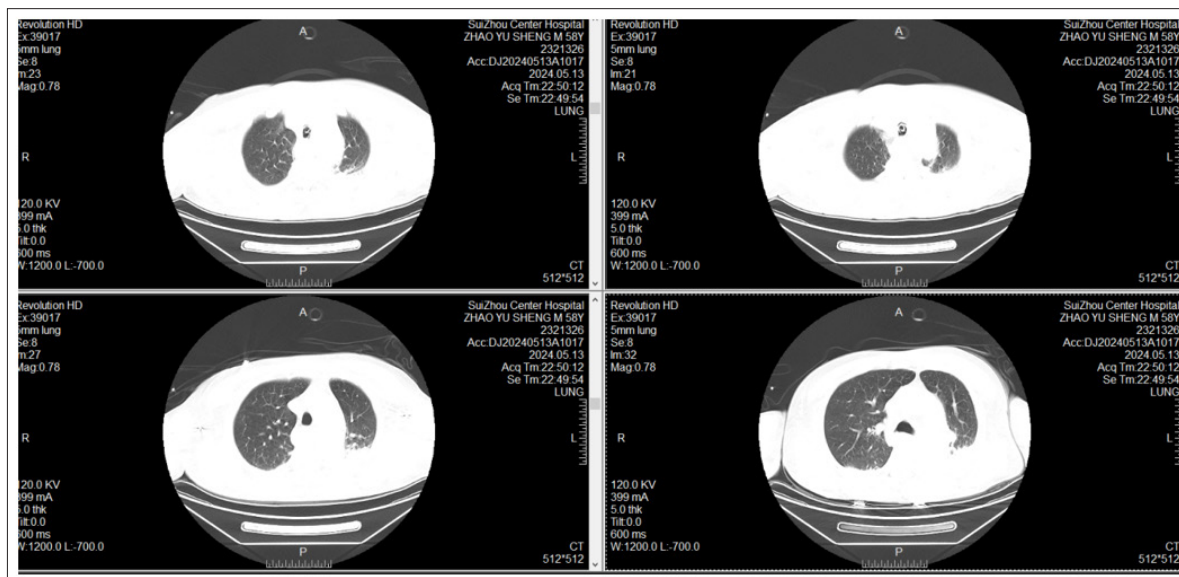


Figure 11: Lung CT on May 13 showed multiple ground glass nodules in the lower lobes of both lungs, with no obvious nodules

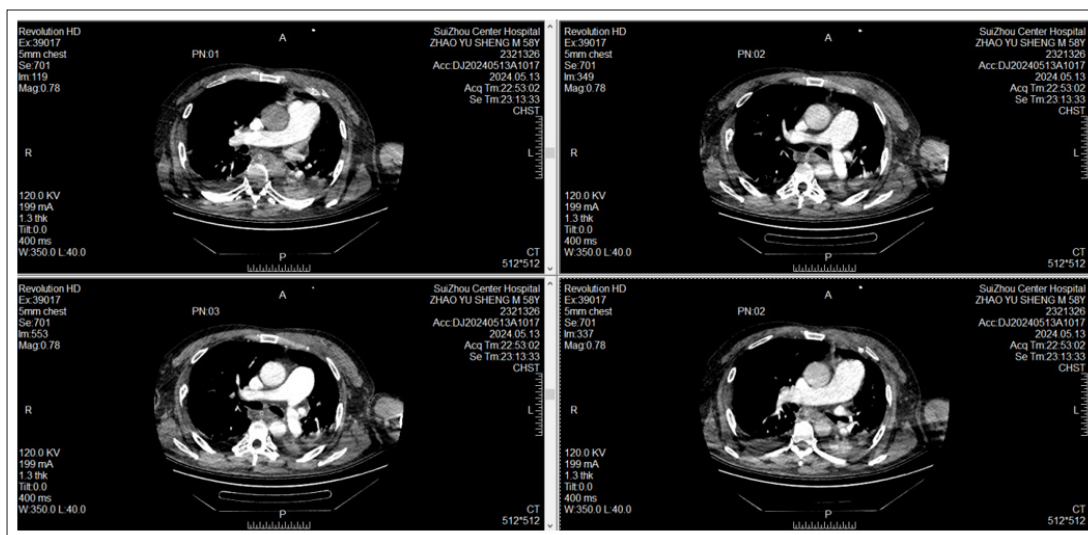


Figure 12: Pulmonary CTA on May 13 suggested embolism in the right upper pulmonary artery branch. Thickened main pulmonary artery (about 3.3cm). (Poor display of double pulmonary artery branches, recommended review)

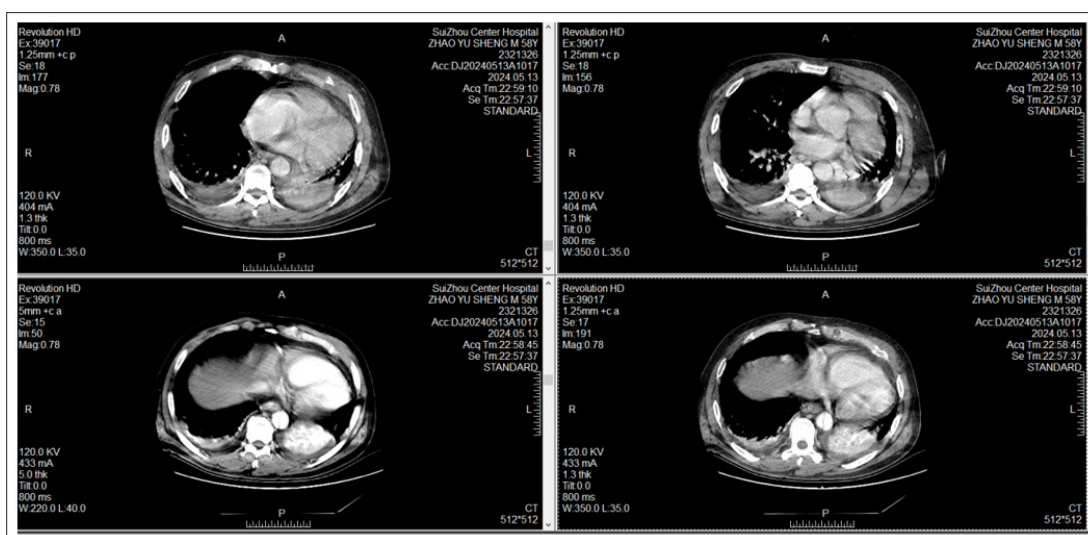


Figure 13: CTA+ 3D reconstruction + 3D imaging of the thoracic and abdominal aorta on May 13 showed that aortic dissection (type III), the abdominal cavity may stem from the false lumen, the right renal artery may originate from the true lumen, the superior mesenteric artery and the left renal artery straddle the true and false lumen, the slightly low density shadow around the superior mesenteric artery was considered to be interwall hematoma, the aortic arch changes were considered to be ulcerated, and small ulcers formed at the beginning of the descending aorta. Please consider clinical review. Atherosclerosis of abdominal aorta, bilateral common iliac artery and internal iliac artery. Cardiothoracic vascular surgery and interventional consultation should be given temporary anticoagulation treatment.

Discussion

Fat embolism syndrome, albeit rare, is associated with a high mortality rate. Without prompt intervention, acute dyspnea and potentially cardiac arrest may manifest within 12 to 72 hours of onset [1-6]. The precise etiology of this syndrome remains elusive [7]. It is postulated that following long bone fractures, fat particles gain access to the systemic circulation and traverse the pulmonary artery and heart, ultimately entering the cerebral arterial system (via ventricular septal defects or a patent foramen ovale), thus precipitating cerebral fat embolism syndrome. The classic triad of fat embolism syndrome is not typically attributed to chest trauma, manifesting as respiratory symptoms such as shortness of breath and dyspnea. Neither is it solely associated with head trauma, presenting with varying degrees of neurological symptoms ranging from headache, agitation, lethargy, convulsions, to coma. Furthermore, hemorrhagic spots often appear in non-dependent areas of the skin and mucous membranes. The symptoms are nonspecific, and chest CT often reveals diffuse ground glass opacity, with “snowstorm-like” changes when lesions are widespread, a characteristic finding in fat embolism. In DWI imaging, high-signal lesions resembling stars against the dark background of brain tissue have been observed, leading some scholars to refer to this as the “starry sky sign” [7, 9].

In the case of multiple trauma, patients frequently exhibit non-specific symptoms such as head and chest trauma, dyspnea, and skin and mucosal bleeding. Lung CT and craniocerebral CT play a definitive role in diagnosis. Here, the patient sustained severe trauma to the right lower extremity. Upon admission on May 9, a lung CT revealed multiple ground-glass nodules, which subsequently

disappeared on May 10. Additionally, the pulmonary artery was noted to be slightly dilated. Postoperatively and following blood transfusion, a craniocerebral CT performed on May 10, the second day of treatment, demonstrated a flaky low-density shadow in the left occipito-parietal lobe, unrelated to the patient's brain trauma or hypotension. Color Doppler ultrasound revealed numerous regurgitant signals during tricuspid valve systole, indicating an enlarged right atrium with a transverse diameter of approximately 41mm. A subsequent CT scan showed significant dilation of the pulmonary artery. Notably, there was no overt venous thrombosis in either lower limb, yet the deep veins exhibited a hypercoagulable state. Given the patient's presentation upon admission, a diagnosis of pulmonary embolism, likely due to fat embolism, was considered. A subsequent pulmonary CTA confirmed embolization of the right upper lobe pulmonary artery branch, along with a thickened main pulmonary artery, approximately 3.3cm in diameter. Notably, the extent of pulmonary thrombus did not correlate with the degree of main pulmonary artery thickening. Thus, a clear diagnosis of fat embolism in this patient was established.

Based on the medical imaging and clinical findings, the patient's diagnosis of aortic dissection type III is clear. On May 9, the mediastinal CT scan revealed calcification in the descending aorta and suspected endometrial shedding, raising the question of whether the aortic dissection was trauma-induced or a pre-existing condition. Further analysis of the patient's injury process is ongoing. On May 10, a CT scan confirmed the presence of calcification in the descending aorta, suspicious dissection, and effusion and hematoma in the lower abdomen and pelvis. These findings were not attributed to bleeding from the liver or kidneys. On May 13, when the patient developed severe abdominal distension, a CTA+3D reconstruction+3D imaging of the thoracic and abdominal aorta was performed. This revealed aortic dissection type III, with the abdominal cavity likely stemming from the false lumen. The right renal artery originated from the true lumen, while the superior mesenteric artery and left renal artery straddled both the true and false lumen. An interwall hematoma was observed around the superior mesenteric artery, and the aortic arch was noted to have ulceration. Small ulcers were also seen at the beginning of the descending aorta. The severe intestinal ischemia leading to abdominal distension was attributed to insufficient blood supply to the patient's superior mesenteric artery due to the dissection. On May 13 and 14, the patient developed aggravated infection, likely caused by intestinal ischemic necrosis and intestinal mucosal necrosis resulting from the tear in the superior mesenteric artery with inadequate blood flow. The possibility of infection at other sites There are two violent forms of traumatic aortic injury. The first is an impact crush injury, which leads to a sudden rise in intrathoracic pressure. The second is a rapid deceleration injury, resulting in a scissor force being applied to the aortic isthmus, specifically in the region between the relatively mobile aortic arch and the relatively fixed descending aorta. As you've noted, approximately 89% of these aortic injuries occur in the aortic isthmus, while other aortic injuries are typically seen in the aortic hiatus and the origins of large vessels. This information is crucial for understanding the mechanisms and locations of traumatic aortic injuries. s could not be excluded.

The patient's condition was complex, involving an aortic dissection type III primarily located in the aortic hiatus. The CTA scan revealed atherosclerosis in the abdominal aorta, bilateral common iliac artery, and internal iliac artery. There is a possibility

that the patient had a pre-existing aortic dissection III, and the trauma sustained may have served as an aggravating factor. On May 13, the CTA further indicated the presence of pulmonary embolism in addition to the aortic dissection III. Despite administering anticoagulant treatment following cardiothoracic surgery and interventional consultation, the patient's abdominal aortic dissection and mesenteric artery insufficiency remained unresolved. Ultimately, the patient succumbed to infection. This case highlights the criticality of early diagnosis and intervention in patients with aortic dissection and associated complications.

Cases involving both fat embolism and aortic dissection type III due to multiple trauma are indeed rare, posing significant challenges in treatment and often resulting in a poor prognosis. The complexity of these injuries, coupled with their rarity, demands a high level of medical expertise and swift intervention to optimize patient outcomes.

Declaration of interest

Ethics Approval and Consent to Participate

We confirm that the manuscript has been read and approved by all named authors and that there are no other persons who satisfied the criteria for authorship but are not listed. We further confirm that the order of authors listed in the manuscript has been approved by all of us.

Consent for Publication

We confirm that we have given due consideration to the protection of intellectual property associated with this work and that there are no impediments to publication, including the timing of publication, with respect to intellectual property. In so doing we confirm that we have followed the regulations of our institutions concerning intellectual property.

Availability of Data and Materials

The datasets used or analysed during the current study are available from the corresponding author on reasonable request.

Competing Interests

The authors declare no competing non-financial/financial interests.

Funding

Not applicable.

Authors Contributions

HHH conceived and designed the study, obtained and interpreted data, performed the statistical analysis, and drafted the manuscript. QZ analysed data and revised the manuscript. XCW obtained data and revised manuscript. JPW revised the manuscript; HHH revised the manuscript. HHH designed the study and revised the manuscript. All authors read and approved the final manuscript.

Acknowledgements

I would like to express my gratitude to all those who helped me during the writing of this thesis. I would like to express my heartfelt gratitude to professor Xiaocong Wang, who led me into the world of translation. And she contributed significantly to analysis and manuscript preparation; last my thanks would go to my beloved family for their loving considerations and great confidence in me all through these years. I also owe my sincere gratitude to my friends and my fellow classmates who gave me their help and time in listening to me and helping me work out my problems during the difficult course of the thesis.

References

1. Ostlie A, Gilbert M, Lewis C (2022) Fat embolism syndrome with neurological involvement: A case report. *J Trauma case reports* 38: 100607.
2. Kassimi, M (2022) "Cerebral fat embolism syndrome after long bone fracture: A case report. " *Radiology case reports* 17: 283-285.
3. Filippatou AG, Naveed M, Barry DP (2021) Sickle cell disease and fat embolism: a rare complication of vaso-occlusive crisis. *J Practical neurology*, 22: 410-412.
4. Hirata Y, Inokuchi G, Tsuneya S (2022) A case of fatal fulminant fat embolism syndrome following multiple fractures resulting from a fall. *J Journal of forensic sciences* 67: 2115-2121.
5. Shafi A, Kar T A, Thoker A B (2022) Fat embolism syndrome: a case series and review of literature. *J International Journal of Research in Medical Sciences* 10: 2005-2010.
6. Guo P, Rao T, Han W (2023) Use of VA-ECMO successfully rescued a trauma patient with fat embolism syndrome complicated with acute heart failure and acute respiratory distress syndrome. *J World Journal of Emergency Medicine* 14: 332-334.
7. Dwivedi S, Kimmel L A, Kirk A (2022) Radiological features of pulmonary fat embolism in trauma patients: a case series. *J Emerg Radio* 1 2: 41-47.
8. Huang CH, Hsieh MH (2021) Isolated cerebral fat embolism syndrome: an extremely rare complication in orthopaedic patients *J ANZ J Surg* 91: 2211-221.
9. Kamel H, Roman MJ, Pitcher A (2016) "Pregnancy and the Risk of Aortic Dissection or Rupture: A Cohort-Crossover Analysis." *Journal of Vascular Surgery* 64:1527-1527.

Copyright: ©2024 Huihua HU, et al. This is an open-access article distributed under the terms of the Creative Commons Attribution License, which permits unrestricted use, distribution, and reproduction in any medium, provided the original author and source are credited.